AUT Journal of Mechanical Engineering

AUT J. Mech. Eng., 9(2) (2025) 123-142
DOI: 10.22060/ajme.2025.23303.6120

# Optimization of cooling system of circular to rectangular transition duct in a turbine engine nozzle

Behrooz Shahriari [1] *, Mojtaba Dehghani[1], Parviz Hashemi[1], Mojtaba Mohamad Hassanzade[2]

[1] Faculty of Mechanics, Malek Ashtar University of Technology, Isfahan, Iran.
[2] Faculty of Aerospace, Malek Ashtar University of Technology, Tehran, Iran.

**ABSTRACT:** This research focuses on optimizing the cooling system of a circular-to-rectangular transition duct in a turbine engine nozzle, a critical step in enhancing engine efficiency by enabling higher turbine inlet temperatures and increased thrust through afterburner usage, both of which significantly elevate exhaust gas temperatures. The study employs a combined film and impingement cooling method and utilizes fluent computational fluid dynamics software for analysis and optimization. Experimental design methodology was used to identify key parameters for optimizing the geometry for three blowing ratios (0.5, 1, and 1.5). Simulation results demonstrate that the optimal cooling configuration for all blowing ratios includes three rows of film cooling. The most influential parameters on cooling efficiency were found to be the diameter of the film cooling holes and the number of film cooling rows. For a blowing ratio of 1.5, increasing the hole diameter and the number of cooling rows resulted in a 32% and 33% increase in cooling efficiency, respectively. Regarding the relationship between cooling angle and efficiency, it was observed that efficiency increased up to 20 degrees and then decreased in blowing ratios of 0.5 and 1.5, while in a blowing ratio of 1, efficiency increased up to 30 degrees and then decreased. This research provides valuable insights into optimizing the cooling system of turbine engine nozzles, enabling more efficient and powerful engines.

**Review History:**

Received: Jun. 27, 2024
Revised: Oct. 23, 2024
Accepted: Dec. 23, 2024
Available Online: Jan. 14, 2025

**Keywords:**

Air Turbine Engine
Rectangular Nozzle
Transition Duct
Combined Cooling
Cooling Efficiency

## 1- Introduction

One of the most common ways to increase efficiency is to raise the temperature in the combustion chamber and then raise the inlet temperature of the turbine engines. The amount of this temperature increase depends on the tolerance of the materials used in the structure of the hot parts of the engine. To increase temperature tolerance, researchers have developed new heat-resistant materials capable of withstanding higher temperatures and are simultaneously developing advanced cooling methods for hot engine components. For this reason, in addition to improving the thermal capacity of materials and using thermal coatings, effective cooling techniques should be used to obtain acceptable life and performance of turbine engine components under thermal loads. With the recent increase in inlet temperatures of turbine engines, new cooling technologies have been implemented. Sometimes, the inlet temperature of certain turbine engine components exceeds the melting point of their constituent materials. This makes the cooling of turbine engine components particularly important. In the analysis of the cooling of the combustion chamber and nozzle, the choice of cooling method and other topics related to the double-walled combustion chamber are considered important requirements in the analysis [1].

Various types of cooling methods are available, including convective cooling, impingement cooling, film cooling, effusion cooling, transpiration cooling, radiation cooling, combined convective-impingement cooling, impingement-film cooling, and film-convective cooling. Convective cooling represents one of the most straightforward cooling techniques, commonly employed for cooling turbine guide blades. Moreover, this method is often employed in conjunction with other techniques, such as film cooling, to effectively cool the combustion chamber. In the impingement cooling method, cool air is introduced through one or more rows of perforations positioned ahead of the cooling surface, where it impinges upon the surface, dissipating its thermal energy. Impingement cooling is a type of convective cooling and its main difference is that the flow hits the surface vertically. The impingement cooling method stands out as an effective and efficient cooling technique employed to safeguard the combustion chamber and nozzle within turbine engines.

In the film cooling method, the basis of the cooling process can be attributed to the creation of a secondary fluid film between the protected wall and the flow of hot gases passing over it, so that the said layer isolates the wall. Over time, the cooling layer undergoes mixing with the main gases and experiences heating from the hot gases, resulting in a rapid decrease in cooling effectiveness downstream.

*Corresponding author's email: shahriari@mut-es.ac.ir

Copyrights for this article are retained by the author(s) with publishing rights granted to Amirkabir University Press. The content of this article is subject to the terms and conditions of the Creative Commons Attribution 4.0 International (CC-BY-NC 4.0) License. For more information, please visit https://www.creativecommons.org/licenses/by-nc/4.0/legalcode.

Typically, to maintain optimal cooling performance, gaps are spaced approximately 4 to 8 cm apart. They are embedded along the surface. The main advantage of this method is that with the penetration of cooling air into the boundary layer, a protective layer is formed along the surface, which protects the surface from hot gases and prevents its corrosion by hot gases. Another important feature is that the injection slots can be designed in such a way that they are resistant to the compressive and thermal stresses caused by high temperatures for long working periods (more than a thousand hours). Also, this method is superior to other methods in terms of simplicity and low cost of the manufacturing process. Furthermore, since no additional components are introduced to the cooling system in this method, concerns regarding added weight are alleviated. The primary limitation of this method lies in its inability to achieve a uniform temperature distribution along the wall. Consequently, the coolest regions are found adjacent to the gaps, with temperatures gradually increasing in the downstream direction ]2[.

Transpiration cooling method, the surfaces are made of porous materials that the cooling air passes through these porous materials and woven materials to the boundary layer to form an insulating film of relatively cool air. This technique is suitable for when the inlet temperature exceeds 1800 K. For effective cooling in this method, the pores should be small. However, reducing the size of the pores may lead to their obstruction by oxidation and foreign particles. Effusion cooling is also more practical than film cooling, which is more advanced and efficient, as well as transpiration cooling, and is used for the temperature range of 1560-1800 K. Ideally, the individual holes should be large enough to prevent clogging by impurities and small enough to prevent excessive penetration of air jets.

Because a large part of heat transfer is related to radiation, groove cooling can partially reduce the cooling load of the inner wall of the liner. In transpiration cooling and effusion cooling systems with multi-layer walls, there exists the potential for clogging of slots and holes by soot particles. Radiation cooling can be used for the nozzle of turbine engines that work in a vacuum. In such cases, the coolant enters the collector, which is located at a distance from the end of the nozzle. In this case, the length of the cooling path is reduced and the hydraulic losses are also reduced. In radiation cooling, the chamber and the nozzle are made of a single wall with heat-resistant materials. Usually, this wall turns red or white, and heat is released into the environment. Radiation cooling is commonly employed in single-fuel propellant chambers, liquid fuel systems, and turbine engines, as well as in divergent nozzle and rocket exhaust components. In this method, heat is dissipated from the external surface of the combustion chamber wall to the surrounding environment. This heat transfer is significant when the temperature difference between the object and the environment is large. In a lower temperature difference, the amount of radiation effect is ignored. To increase the radiation heat transfer from the object to the environment, the emission coefficient of the object must be high. This cooling method finds application in compact combustion chambers featuring materials capable of withstanding elevated temperatures, particularly in regions characterized by low heat flux ]3[.

In the combined impingement-convective cooling method, the middle part of the blade is cooled through horizontal ducts in the form of displacement, and the leading edge is cooled through impingement cooling. Air flows upwards inside the central cavity. The outer wall of this cavity consists of a series of horizontal channels and there are many holes at the edge of its attack. Following the cooling process, the airflow through these apertures impacts the leading edge of the vane within the horizontal channels formed between the wall and the shell, subsequently exiting through the gap at the trailing edge. By employing this method, we capitalize on the benefits offered by both cooling techniques. In the combined film-impingement cooling method, the air flows upwards inside the central cavity. The outer wall of this cavity consists of a series of horizontal channels and there are many holes at the edge of its attack. Following the cooling of the leading edge of the vane, air exits through the film cooling holes, providing cooling to the remainder of the vane surface via film cooling. This method has a higher cooling efficiency than the combined impingement-convective cooling method.

In the film-convective method, the middle area of the blade is cooled by convective, and the leading edge is cooled by both convective and film. The air required for cooling is injected from the blade base towards the central cavities. At the leading edge, the air passes through the holes related to film cooling, and the trailing edge is cooled by convective air from the gap.

The investigation into impingement-film cooling was initially conducted by Metzger and Bunker [4] in 1990. They used one impingement cooling row in the blade leading edge model and two cooling rows in the suction region and the pressure region of the blade near the leading edge. Their results show that heat transfer is dependent on the alignment of the impingement cooling row concerning the film cooling row. In 1995, Garg and Gaugler [5] studied the effect of velocity and temperature distribution in the jet outlet on the film cooling of turbine blades. For this purpose, they used the adjusted polynomial and 1/7 power and temperature profiles. Their results show that the speed and temperature profile at the jet outlet can change the heat transfer coefficient by up to 60%. Walters and Leylek [6] in 1997, numerically studied the film cooling problem using the Fluent code. In their study, they also addressed the flow dynamics within the jet channel and the plenum as integral components of the computational domain. They used the unorganized network to generate the network for the above complex computational domain and used high-order methods to separate the equations.

In 1999, Baldauf et al. [7] studied the cooling efficiency experimentally. Their findings indicate that the maximum cooling efficiency values at various blowing ratios are achieved at different distances downstream from the holes. This variation can be attributed to the phenomenon of air detachment from the surface at initial distances followed by reattachment downstream. Kaszeta and Simon [8], in their

2000 analysis of compound angle injection, concluded that injecting cooling compounds in both lateral and perpendicular directions to the wall yields superior results compared to injection at a single angle. They demonstrated that at blowing ratios exceeding one, lateral injection increases the likelihood of the jet lifting from the surface, resulting in an enhanced heat transfer coefficient. They also showed that in lateral injection, due to the larger spread of the gradient, the total velocity decreased and, as a result, the reduction in shear stresses will result. In 2002, Tehrani and Mahmoodi [9] investigated the effect of injection angle and turbulence intensity in film cooling in three dimensions using the finite element method. Their results show that the best cooling air injection angle for a film cooling hole is 35 degrees. Zecchi et al. [10] in 2004 designed a cooling system for a gas turbine. The study of the overall cooling efficiency of the vane turbine was experimentally conducted for the first time by Albert et al. [11] in 2004. They conducted experimental studies on the adiabatic efficiency and overall cooling efficiency for blades equipped with film cooling. In this research, a model of the leading edge of the blade incorporating three rows of cooling holes was employed. To study the adiabatic efficiency, a model with a low conductivity coefficient was used, and to study the overall efficiency, a model whose Biot number was equal to the real sample was used. Their results show a clear difference between adiabatic efficiency and total efficiency. Ghorab et al. [12] in 2008, investigated multi-stage cooling on a flat plate through simultaneous numerical analysis of heat transfer. They investigated the effect of parameters such as the geometry of the holes and the distance to the target surface. Their results show that increasing the distance between the jet nozzle and the target surface increases the heat transfer, but due to the increase in the cooling air temperature at this stage, the film cooling efficiency decreases.

In 2009, Dobrowolski et al. [13] Numerical analysis was employed to study a model of the blade's leading edge featuring film-impingement cooling. They used simultaneous heat transfer analysis to predict the dimensionless temperature of the blade surface. Simultaneously, the adiabatic efficiency and overall efficiency of this sample were experimentally determined. They used $K-\varepsilon$ Realizable turbulence model to analyze the flow. The numerical results of adiabatic efficiency are in good agreement with the experimental results. However, the local efficiency along the trajectory of the airflow downstream of the holes predicts larger values, attributed to the inadequate analysis of the model in the separation regions. The trend of changes in numerical values of overall efficiency is in accordance with the experimental results, but in the stagnation region, it shows larger values than the experimental values. In this study, because the experimental test and numerical simulation were done in the same laboratory, all the experimental conditions needed to create accurate boundary conditions were included in the numerical simulation.

In 2010, Ravelli et al. [14] numerically investigated the effect of using impingement cooling in cooling the front edge of the blade. They investigated the effect of cooling hole diameter and location of impingement cooling hole row. Their results show that the use of an impingement cooling row does not have much effect on increasing the overall cooling efficiency. Also, reducing the diameter of the cooling hole when the cooling air flow rate is constant does not make a noticeable change in the overall efficiency. In 2014, Suresh et al. [15] conducted studies on the flow and heat transfer of rotor blade cooling. A military gas turbine engine operates at a turbine inlet temperature (TET) of about 2000 K. Increasing TET improves thermal efficiency and power output. The gas temperature is much higher than the permissible metal temperature of the turbine components. Hence, there is a need to cool components such as blades and vanes for safe operation. The blades undergo cooling through a combination of convective cooling and external film cooling. In order to model the external flow, empirical correlation relations have been used based on the calculation of the displacement heat transfer coefficient of the external surface. Blade temperature distribution has been extracted by finite element software. In 2016, Klavetter et al. [16] experimentally investigated the effect of the presence of a notch on the surface (including the cooling hole). They obtained the adiabatic cooling efficiency for the channel including film cooling with the notch on it (the cooling hole and the notch are on the same surface). 8 different modes were investigated according to the orientation of the notch in relation to the cooling airflow and the location of the cooling holes in relation to the notch. Their results indicate that the condition of the inlet flow to the cooling hole significantly impacts cooling efficiency, and employing obstacles to disrupt the flow can enhance cooling efficiency. In 2016, Wang et al. [17] numerically investigated the efficiency of film cooling with a notch on a flat plate. They investigated the impact of surface indentation, incorporating film cooling, through simultaneous heat transfer analysis. Their results indicate that incorporating a notch on the surface, along with film cooling while maintaining a constant cooling flow, can enhance the efficiency of film cooling.

In 2019, Zhao et al. [18] investigated radiant coolers. Radiation cooling has attracted much attention in the energy field as a passive, effective, and renewable method to reduce cooling energy requirements without power input. In 2020, Andrii et al. [19] conducted studies on turbine inlet air cooling systems. The cooling efficiency of ambient air at the inlet of gas turbines in moderate weather conditions has been analyzed. A new trend has been achieved in cooling the intake air to the engine by 7 or 10°C in mild climates with two-stage cooling in combination chillers that provide annual fuel savings of up to 50%.

In 2021, Thomas et al. [20] studied the combined impingement-effusion cooling of the combustion chamber liner. The inner wall on the hot gas side has an effusion cooling system and the outer wall on the cold side has a pattern of collision holes with circular holes. A test device has been used to evaluate the aerodynamic and thermal behavior. Temperature data are obtained using two infrared systems on either side of the effusion sample. In addition to evaluating the cooling efficiency, finite element simulations have been

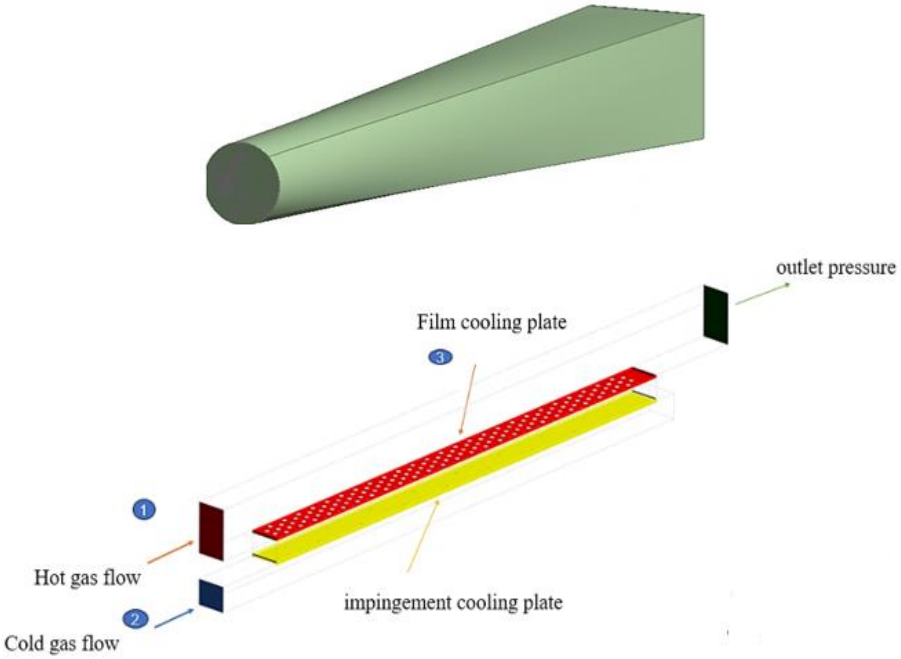


**Fig. 1. 3D geometry of the transition duct (right side) and the strip used to achieve the optimal geometry (left side)**

done. The results show that the cooling efficiency of the hot gas side can reach above 90% and is mainly affected by the effusion coating, and the impingement cooling has little effect on the overall efficiency. Fan et al. [21] in 2022 investigated the concepts of photonics and thermodynamics in cooling. Radiation cooling is a passive process that uses photon heat flow to transfer energy and entropy. Radiation cooling processes have been studied in the scientific literature for decades, but advances in nanophotonics have enabled recent advances in daytime radiation cooling. Radiation cooling is now emerging as a frontier in renewable energy research with significant potential for a wide range of applications. This review delves into the fundamental principles of photonics and thermodynamics, serving as the foundation for understanding radiation cooling processes. Yuhao et al. [2] in 2023 studied numerically the efficiency of film cooling in spiral channels. Due to its better performance, film cooling has attracted much attention.

Robert et al. [3] in 2023 conducted a study on the applications of impingement cooling. One of these applications is the cooling of electronic components. The purpose of this article is to reduce heat transfer in electronic components. In 2023, Jian et al. [22] analyzed the impingement cooling flow (film and impingement) in a double-walled surface. This article investigates the influence of the angle of incidence, blowing ratio, and Biot's number on conjugate heat transfer. The results show that by increasing the collision angle from 15 to 30 degrees, the cooling efficiency has increased by about 20%, and also increasing the blowing ratio increases the cooling efficiency.

A review of the conducted research suggests that film-impingement cooling exhibits higher cooling efficiency. Additionally, the computational fluid dynamics (CFD) method proves effective in accurately predicting nozzle cooling. The K-ω SST turbulence model has been predominantly utilized in numerical simulations to enhance the prediction of flow properties.

In modern turbine engines, various cooling systems are used to increase engine efficiency in the hot parts of the engine. The objective of this research is to analyze and design a duct cooling system for converting the circular cross-section into a rectangular shape at the inlet of a turbofan engine nozzle. In rectangular nozzles, the inlet section of the nozzle comprises a transition duct, which connects the circular section of the afterburner to the rectangular nozzle. Due to the location of the transition duct immediately after the afterburner, this part experiences a very high temperature and its cooling is important as an important part of the nozzle.

## 2- Numerical modeling

In this article, the design of the cooling system of the circular to rectangular transition duct at the inlet of the nozzle of a turbine engine has been discussed using numerical simulation. Fig. 1 shows the three-dimensional geometry of the transition duct. Due to the complexity of the transition duct geometry, only a narrow strip has been used for simulation. The geometry used for the cooling design can also be seen in Fig 1. The geometry used includes combined (film-impingement) cooling. The flow of hot gas with a temperature of 2100 K is entered from number 1 and the flow of cold gas with a temperature of 430K is entered into the geometry. The cold gas stream is used to cool plate number

**Table 1. Range of input parameters**

| Parameter | Symbol | Min | Max |
|---|---|---|---|
| Blowing ratio | $M$ | 0.5 | 1.5 |
| The angle of the film cooling holes | $\theta$ | 30 | 90 |
| Diameter of film cooling holes | $d_f$ | 0.5 | 2 |
| Diameter of impingement cooling holes | $d_i$ | 0.5 | 2 |
| The number of film cooling rows | $N$ | 1 | 3 |
| The distance between the two impingement cooling plates and the film | $h$ | 10 | 30 |
| Center-to-center distance of film cooling holes | $f_i$ | 8 | 16 |

3. The cooling fluid first passed through the impingement cooling plate, then entered the geometry through the cooling holes of the film embedded on the flat plate and caused the formation of a boundary layer of cold gas flow on the flat plate, and from the direct contact of the hot gas flow with the plate Smooth has prevented. The working fluid utilized in this study is air (considered as an ideal gas). To enhance the thermal and fluid transfer performance of the transition duct, an optimization method employing genetic algorithms has been employed.

In every problem, the first step for optimization is to determine the input and output parameters. Subsequently, the input parameters to be optimized, as well as the corresponding output parameters, will be determined during the optimization process. In the present problem, the input and output parameters are defined first. These input parameters of the problem include two parts: geometric parameters and fluid flow parameters. Also, certain ranges are considered for the input parameters, which can be seen in Table 1 [23]. The geometric input parameters under consideration encompass the angle of the film cooling holes *(θ)*, the diameter of the film cooling holes *(df)*, the diameter of the impingement cooling holes *(di)*, the number of film cooling rows *(N)*, the distance between the two impingement cooling plates and the film *(h)*, and the center-to-center distance of film cooling holes *(fi)*. Also, in this study, the blowing ratio *(M)* is considered as the fluid flow parameter. The blowing ratio, a characteristic parameter of the flow, is a dimensionless quantity representing the ratio of the density product of the cooling flow rate to that of the hot gas flow rate. The output parameter is determined by the cooling efficiency.

In the current study, a compressible, three-dimensional, turbulent, single-phase, and steady flow regime is considered. The fluid analyzed is air, treated as an ideal gas. The application of the law of conservation of mass on the constant control volume establishes the continuity relationship is obtained in the form of Eq.1.

$$\frac{\partial}{\partial x_i}(\rho U_i) = 0 \tag{1}$$

In Eq.1, ρ is fluid density and U is fluid velocity. The first term in this equation represents the rate of mass flux passing through the surface of the control volume per unit volume. By using Newton's second law on the fixed and small control volume through which the fluid passes, the momentum equation becomes Eq.2.

$$\frac{\partial}{\partial x_j}(\rho U_i U_j) = -\frac{\partial p}{\partial x_i} + \frac{\partial}{\partial x_j}(2\mu S_{ij}) + F_i \tag{2}$$

In Eq.2, represents the strain rate tensor and $S_{ij}$ $\mathrm{represents the strain rate tensor, and F_i}$ denotes the volume forces acting on the basal plane, encompassing forces induced by magnetic fields. The strain rate tensor is defined as follows:

$$S_{ij} = \frac{1}{2}\left(\frac{\partial U_i}{\partial x_j} + \frac{\partial U_j}{\partial x_i}\right) \tag{3}$$

Continuity and momentum equations are expressed in a general form. These equations will take different forms according to the flow conditions. For a smooth flow, the above equations can be solved analytically by considering some simplifying assumptions, but in turbulent flows, these equations cannot be solved analytically, and due to the many complexities of the equations, tools are needed for numerical solutions. Considering the law of conservation of energy per unit of constant control volume, the energy equation becomes Eq.4:

$$\nabla.(\vec{\nabla}(\rho E + \mathrm{P})) = \nabla.(K_{eff}\nabla T) + S_h \tag{4}$$

In Eq.4, E is the total fluid energy obtained from Eq.5:

$$E = h - \frac{P}{\rho} + \frac{v^2}{2} \quad (5)$$

Also, in Eq.5, h is fluid enthalpy, which is obtained from Eq.6 based on the definition. In Eq.6, the reference temperature ($T_{ref}$) is considered equal to 298.15 K.

$$h = \int_{T_{ref}}^{T} C_P dt \quad (6)$$

The cooling effectiveness $\eta$ is calculated from Eq.7, where $T_W$ is the wall temperature, $T_\infty$ is the temperature of the main flow and $T_{Jet}$ is the temperature of the outlet jet

$$\eta = \frac{T_w - T_\infty}{T_{jet} - T_\infty} \quad (7)$$

$$M = \frac{\rho_j u_j}{\rho_\infty u_\infty} \quad (8)$$

The blowing ratio is defined according to Eq.8, where $\rho_j$ and $u_j$ are the density and velocity of the jet fluid, and $\rho_\infty$ and $u_\infty$ are the density and velocity of the main flow.

The momentum ratio is defined according to Eq.9, where $\rho_j$ and $u_j$ are the density and velocity of the jet fluid, and $\rho_\infty$ and $u_\infty$ are the density and velocity of the main flow. On the smooth surface, with the increase of the momentum flux ratio, the amount of cooling effectiveness near the injection hole decreases. The reason for that is the increase in penetration of the injection jet in the main stream.

$$I = \frac{\rho_j (u_j)^2}{\rho_\infty (u_\infty)^2} \quad (9)$$

The density ratio is also defined according to Eq.10, where and $\rho_j$ are the density of the main stream and the density of the jet, respectively.

$$D.R = \frac{\rho_j}{\rho_\infty} \quad (10)$$

And finally, the absolute speed ratio is also defined according to Eq.11:

$$V.R = \frac{u_j}{u_\infty} \quad (11)$$

## 3- Results and Discussion

### 3- 1- Validation with experimental testing

For validation with experimental testing, the geometry of Jia et al. [1], who dealt with the cooling of the liner wall, was used, which can be seen in Fig.2. The geometry used has two film-impingement cooling plates. The film-impingement cooling plate includes 72 and 16 holes, respectively. The angle of the impingement cooling and film cooling holes is 90 degrees. The design, meshing, creation of boundary conditions, and fluid definition were performed using the commercial software Ansys Fluent, as depicted in Fig 3. Near the walls, the mesh is refined to ensure that the value of y+

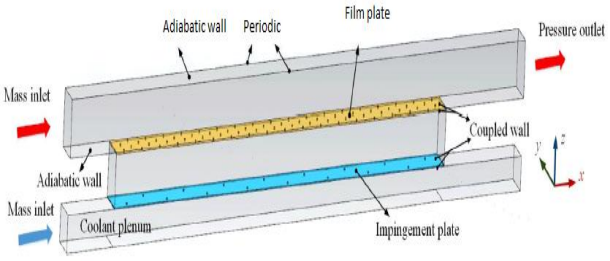


**Fig. 2. 3D geometry and boundary conditions in the current research [1]**

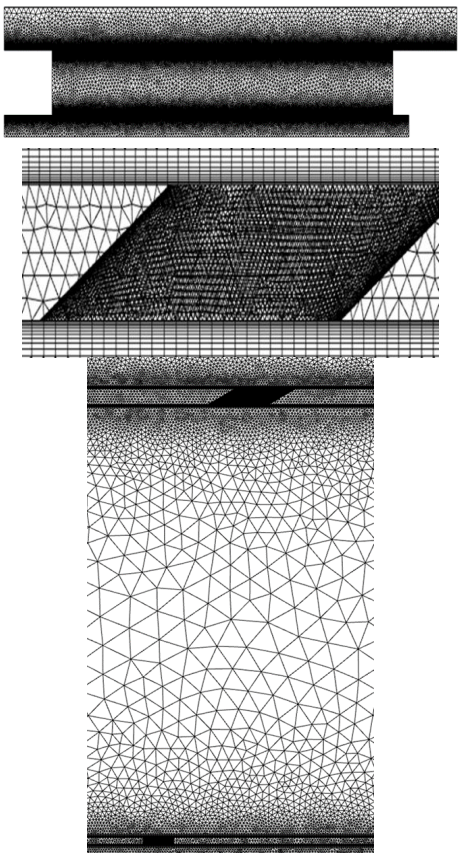

**Fig. 3. A view of the network created with Ansys Machining software**

**Table 2. Information about boundary conditions [1]**

| Boundary conditions | Amounts |
|---|---|
| $T_g$ | 603 K |
| $p_g$ | 101000Pa |
| $\rho_g$ | 0.55 Kg/m$^3$ |
| $\rho_c$ | 1.19 Kg/m$^3$ |
| $T_c$ | 298 K |
| $Re_c$ | 817-6645 |
| $k_s$ | 2.2-10.12 W/m.K |

falls within the permitted range. Additionally, in the vicinity of the holes, where there are significant gradients in the flow field and heat transfer, the mesh is finer.

### 3- 2- Boundary conditions

In this research, 4 boundary conditions are used in the form of inlet flow boundary, pressure outlet boundary, adiabatic wall boundary, and periodic boundary. The lower wall and the upper surface of the channel are assumed to be adiabatic. At the entrance of the primary flow channel, the discharge boundary condition is employed. The temperature of the hot gas flow is equal to 603 K. For the lower surface of the cooling fluid chamber, the constant flow boundary condition is used, where the temperature of the cooling fluid is equal to 298 K and the ratio of the density of the cooling fluid to the density of the hot gas flow is 2.16. In Table 2, the information about the boundary conditions is given.

### 3- 3- Validation results

In this section, the cooling efficiency has been investigated at a blowing ratio of 0.5. As you can see in Fig. 4, the average error rate is 6%, which indicates a good agreement between the results of the numerical solution and the experimental test. During the transition duct, the cooling efficiency initially increases, but as it approaches the end of the duct, it decreases. This decline can be attributed to the heightened temperature gradient at the transition duct's termination.

## 4- The geometric model used to achieve the optimal geometry

To achieve the optimal geometry that has the highest cooling efficiency, the geometries of Fig. 5 have been used for modeling in Fluent computational fluid dynamics software. The geometries used have 1, 2, and 3 film cooling rows, respectively. The lowest and highest number of film cooling holes are for geometries with 1 and 3 rows of film cooling holes, respectively. Also, the parameters of the geometric model are shown in Fig.6. In all the geometries used to achieve the optimal geometry, the angle of the impingement cooling holes is 90 degrees.

Considering the complexity of the flow field in the transition duct, the production of the grid is very important. To investigate the network and verify the robustness of the results, five distinct networks with varying numbers of

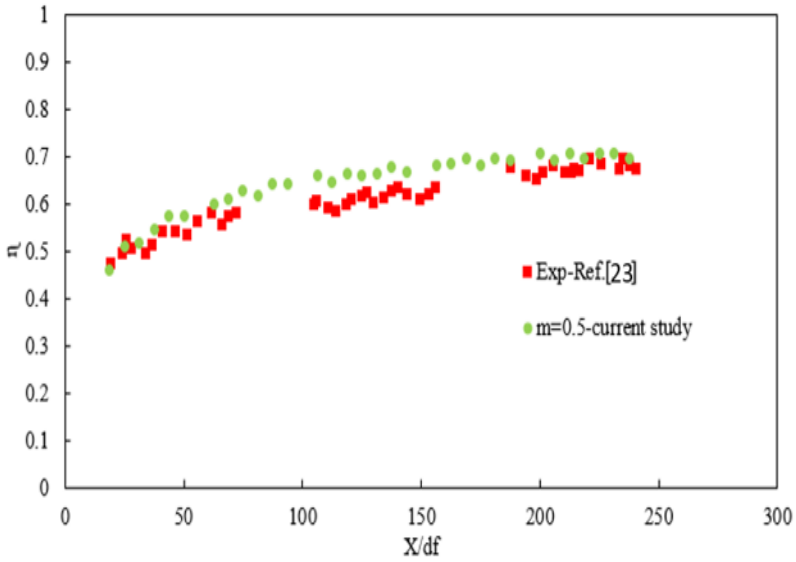


**Fig. 4. Comparing the results with the experimental test**

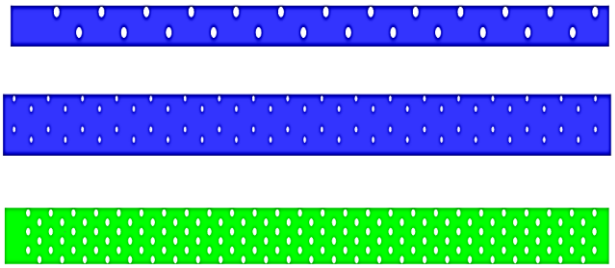

**Fig. 5. The geometric model used for optimization with the number of rows of cooling holes, 2, 1, and 3 rows from the top, respectively.**

cells are analyzed, and the resultant findings are depicted in Fig.7. The considered criterion is the cooling efficiency obtained from the steady state analysis. As shown in Fig.7, the calculated error decreases as the number of grids in the solution domain increases. Indeed, an excessive number of networks can significantly escalate computational expenses. On the other hand, the small number of grids reduces the accuracy of calculations and the lack of observation of flow field phenomena. Therefore, the number of grids should only be greater in areas with gradient flow properties. Therefore, choosing the right number of networks for simulation is of particular importance.

As stated before, in the problem of optimizing heat transfer and fluid flow in a circular-to-rectangular section transition duct at the inlet of the turbine engine nozzle, 7 input parameters are defined; These parameters include 6 geometric parameters and 1 flow parameter. The output parameter, which corresponds to the input parameters specified in the experimental design, has been determined through numerical simulation employing computational fluid dynamics (CFD) methods within the Fluent commercial software. This output parameter encompasses the mean average temperature (Tav) has been extracted. In this section, the optimization results are

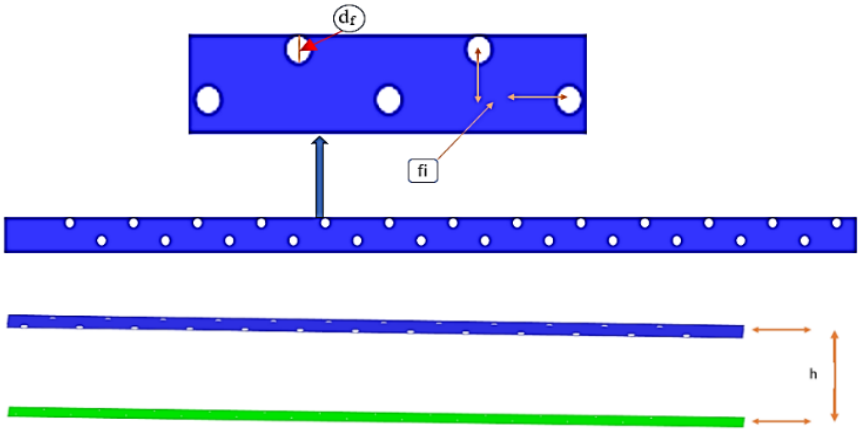


**Fig. 6. The parameters of the grid independence geometric model**

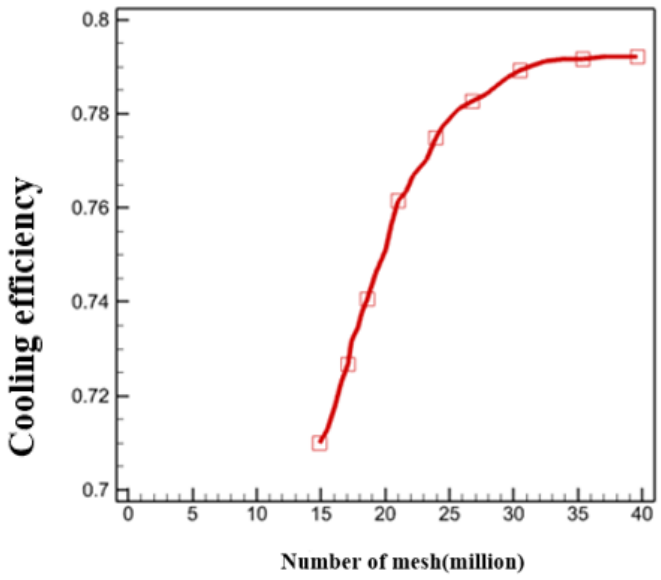


**Fig. 7. Checking the network in the geometric model used to achieve the optimal geometry**

**Table 3. Output parameter for optimal conditions**

| | $T_{Ave}$(K) | | |
|---|---|---|---|
| Blowing ratio | 0.5 | 1 | 1.5 |
| Predictive optimization | 893.57 | 709.45 | 605.82 |
| Numerical simulation | 855.85 | 723.085 | 618.70258 |
| error (percentage) | 4.26 | 1.92 | 2.13 |

**Table 4. Specifications of the optimal geometry with the highest cooling efficiency for the blowing ratio of 0.5**

| $M$ | $N$ | $f_i$(mm) | $h$(mm) | $\theta$ | $d_f$(mm) | $d_i$(mm) |
|---|---|---|---|---|---|---|
| 0.5 | 3 | 12 | 10 | 18 | 1.66 | 0.66 |

presented. As outlined, subsequent to identifying the output parameter at the test points, the genetic algorithm method has been employed to optimize the results. In the optimization process, it is necessary to check the correctness of the output parameter at the proposed point by the genetic algorithm. For this purpose, according to the input parameters of the optimal design point, the output parameter has been obtained using the numerical simulation method for 0.5, 1, and 1.5. These values are presented in Table 3, and the error rate of the output parameter obtained from the genetic algorithm optimization method is compared to that of the numerical simulation method. It can be seen that the error rate is very low and the obtained results are valid for the optimal point.

In Table 4, you can see the specifications of the optimal geometry with the highest cooling efficiency for the blowing ratio of 0.5. The optimized geometry has 3 rows of film cooling holes. The diameter of the film cooling and impact holes are 1.66 and 0.66 mm, respectively. In the optimal geometry, the angle of the film cooling holes is 18 degrees and the distance between the two cooling plates is 10 mm, which has resulted in a cooling efficiency of 74.5.

Fig.8 shows the contour of cooling efficiency distribution on a flat surface for the tail ratio of 0.5. The range of cooling efficiency is between 0.26 and 0.86, which is the minimum and maximum cooling efficiency corresponding to the beginning and end of the flat plate, respectively. As can be seen, at the beginning of the flat plate, the flow of cold gas does not penetrate enough; Therefore, the cooling efficiency at the beginning of the flat plate is small. Then, by approaching the end of the plate and increasing the flow rate of the cooling fluid inlet, the momentum of the cold gas flow increases, as a result of which the cooling efficiency is improved. Additionally, at the trailing edge of the flat plate, the cooling efficiency has diminished, attributed to the amalgamation of the cooling fluid with the hot gas flow.

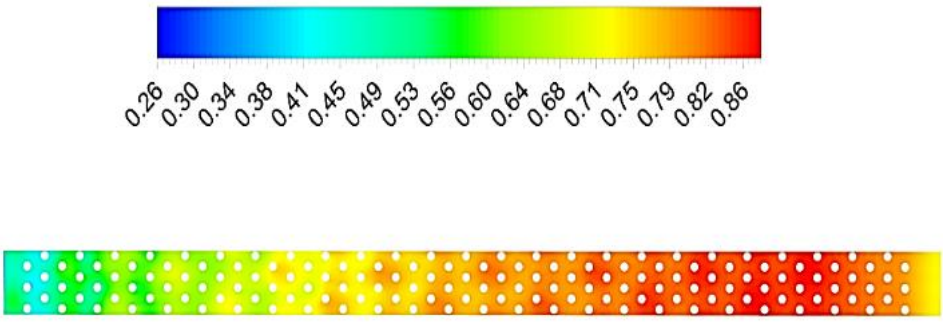


**Fig. 8. Cooling efficiency distribution contour on a flat plate with a blowing ratio of 0.5**

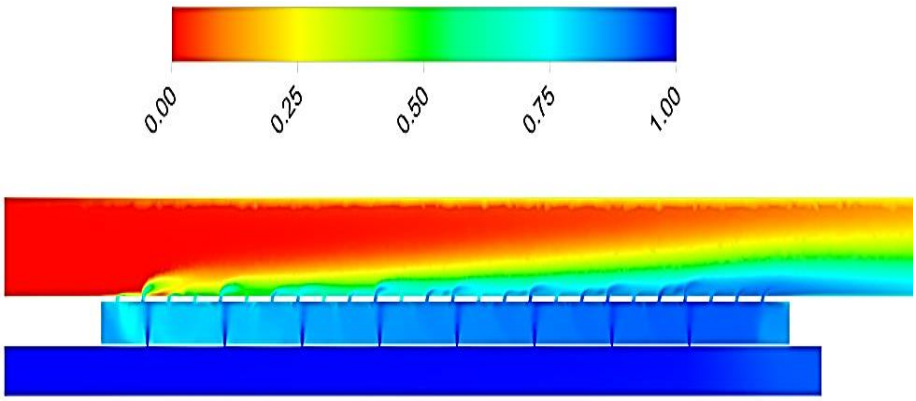


**Fig. 9. Cooling efficiency distribution contour for optimal geometry with 0.5 blowing ratio**

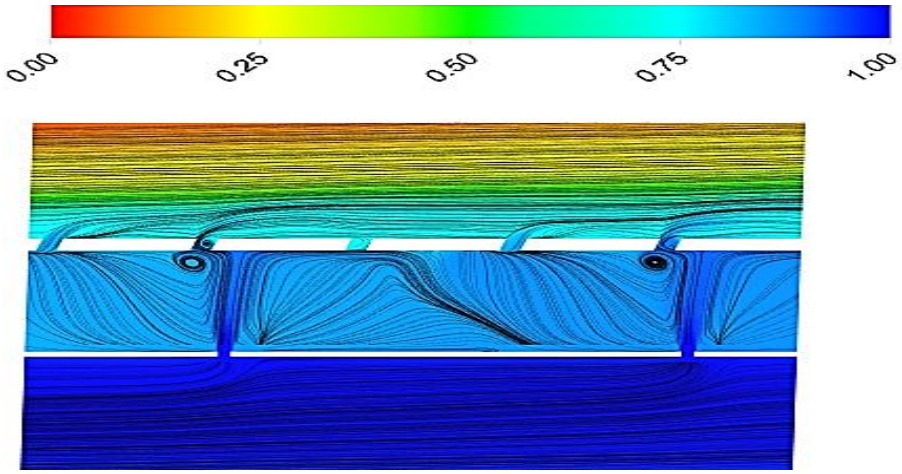


**Fig. 10. Streamline distribution for the optimal geometry with a blowing ratio 0.5**

Fig.9 shows the distribution of cooling efficiency for the optimized geometry with a blowing ratio of 0.5. The angle of the impingement cooling holes is 90 degrees. The cooling fluid enters the hot gas flow through the film cooling holes fixed on the flat plate. The range of cooling efficiency is between 0 and 1. In the vicinity of the injection holes, the cooling efficiency reaches its maximum value. As can be seen, at the beginning of the hot gas flow, the efficiency is zero due to the lack of expansion of the cooling fluid to that area. As the end of the flat plate is approached and the momentum of the cold gas flow increases, effective cooling is achieved, resulting in the attainment of maximum efficiency.

Fig.10 shows the distribution of streamlines for the optimal geometry with a blowing ratio of 0.5. The angle of the impingement cooling holes is 90 degrees. The cooling fluid enters the hot gas stream through the film cooling holes embedded in the flat plate. The range of cooling efficiency is between 0 and 1, which reaches its maximum value in the areas near the hole. As can be seen in the figure, due to the generation of vortices near the cooling holes of the film, the cold gas flow does not penetrate well. The cause of this phenomenon is the decrease in the momentum of the cold gas flow.

Fig.11 shows the sensitivity of the input parameters in terms of the percentage of cooling efficiency ($\eta$) with a blowing ratio of 0.5. As evident, the cooling efficiency ($\eta$) has risen with the increase in three parameters: the diameter of the film cooling holes *(df)* the number of film cooling rows *(N)*, and the blowing ratio *(M)*. Also, the increase in parameters of the diameter of impingement cooling holes *(di)*, the distance between the film-impingement cooling plates *(h)*, the center-to-center distance of the film cooling holes *(fi)* and the angle of the film cooling holes *(θ)* have led to a decrease in the cooling efficiency. The increase of the two parameters of the diameter of the film cooling holes *(df)* and the number of film cooling rows *(N)*, which are caused by the increase in the momentum and the amount of the input flow of the cooling flow, respectively; It has increased cooling efficiency by 30 and 28%, respectively, which have the greatest impact on improving efficiency. Also, the increase in pressure drop

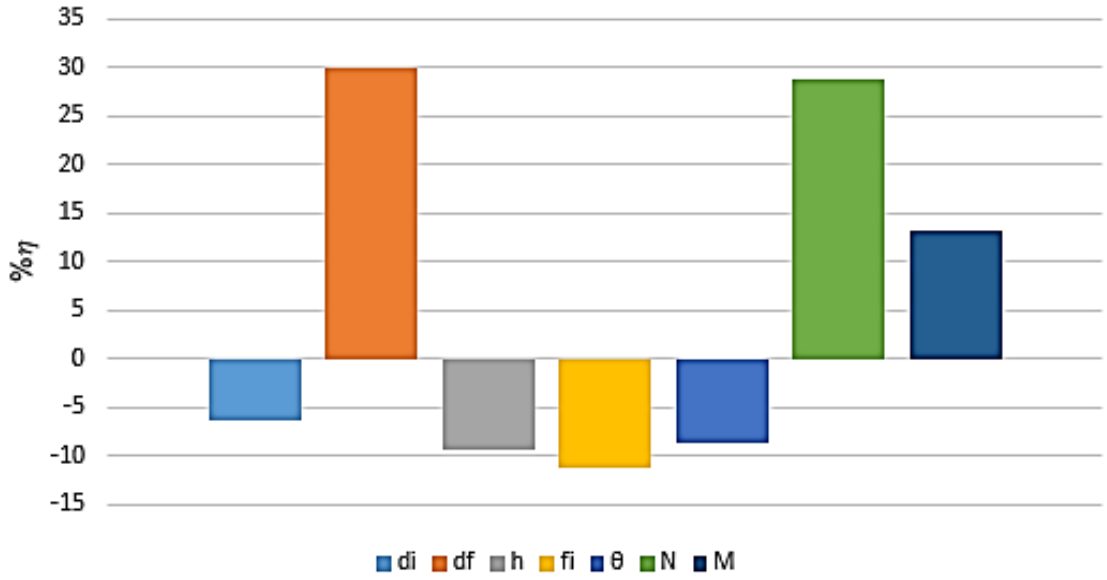


**Fig. 11. The sensitivity of the input parameters on the cooling efficiency for the blowing ratio of 0.5**

created between the cooling holes of the film, which led to an increase in fi, reduced the cooling efficiency by about 11%, which is the most effective parameter on reducing the cooling efficiency.

Fig.12 illustrates the variations in the diameter of the film cooling holes *(df)* and the center-to-center distance of the film cooling holes *(fi)* concerning Tave for a blowing ratio of 0.5. The results of the optimization have predicted a diameter of 1.66 mm for the optimal geometry with a blowing ratio of 0.5. As observed, with the increase in df, both the cooling air flow rate and inlet velocity rise, leading to a decrease in Tave , and consequently, an increase in cooling efficiency. It can also be seen that the optimal center-to-center distance of film cooling holes is 12 mm. As evident, with the increase in fi, Tave rises, leading to a decrease in cooling efficiency. This decline is attributed to the increased pressure drop along the cooling flow path.

Fig.13 shows the changes in the distance between the two film- impingement cooling plates *(h)* and the changes in the film cooling angle *(θ)* in terms of Tave for the blowing ratio of 0.5. The optimization results have forecasted the distance between the two film-impingement cooling plates to be 10 mm for the optimal geometry with a blowing ratio of 0.5. As can be seen, with the increase of h, which leads to the increase of Tave, the cooling efficiency has decreased. The reason for this is the increase in pressure drop along the path of the cooling flow, which has reduced the momentum of the cooling fluid. Furthermore, an optimal cooling angle of 18 degrees has been determined. It is evident that from an angle of 0 to nearly 20 degrees, Tave decreases, consequently leading to an increase in cooling efficiency. The reason for this phenomenon is the retention of the cold gas flow within the boundary layer. Then, with an increase in the angle beyond approximately 20 degrees, Tave increased, leading to a decrease in cooling efficiency. The reason for this decrease is the cooling flow directed out of the boundary layer.

In Table 5, you can see the specifications of the optimal geometry with the highest cooling efficiency for the blowing ratio of 1. The optimized geometry has 3 rows of film cooling holes. The diameter of the film cooling and impact holes are 1.6 and 1.0099 mm, respectively. In the optimal geometry, the angle of the film cooling holes is 14.69 degrees and the distance between the two cooling plates is 11.542 mm, which has resulted in a cooling efficiency of 82.45.

Fig.14 shows the contour of the cooling efficiency distribution on the flat plate for a blowing ratio of 1. The range of cooling efficiency is between 0.30 and 0.92, which is the minimum and maximum cooling efficiency corresponding to the beginning and end of the flat plate, respectively. As observed, at the initial section of the flat plate, the penetration of cold gas flow is insufficient, resulting in a lower cooling efficiency at the onset of the flat plate. Then, by approaching the end of the plate and increasing the flow rate of the cooling fluid, the momentum of the cold gas flow increased, as a result of which the cooling efficiency improved. Similarly, at the trailing edge of the flat plate, the cooling efficiency has diminished. The mixing of the cooling fluid with the hot gas flow is the reason for this phenomenon, as a result of which the power of the cooling fluid has been reduced.

Fig.15 shows the cooling efficiency distribution for the optimized geometry with a blowing ratio of 1. The angle of the impingement cooling holes is 90 degrees. The cooling fluid

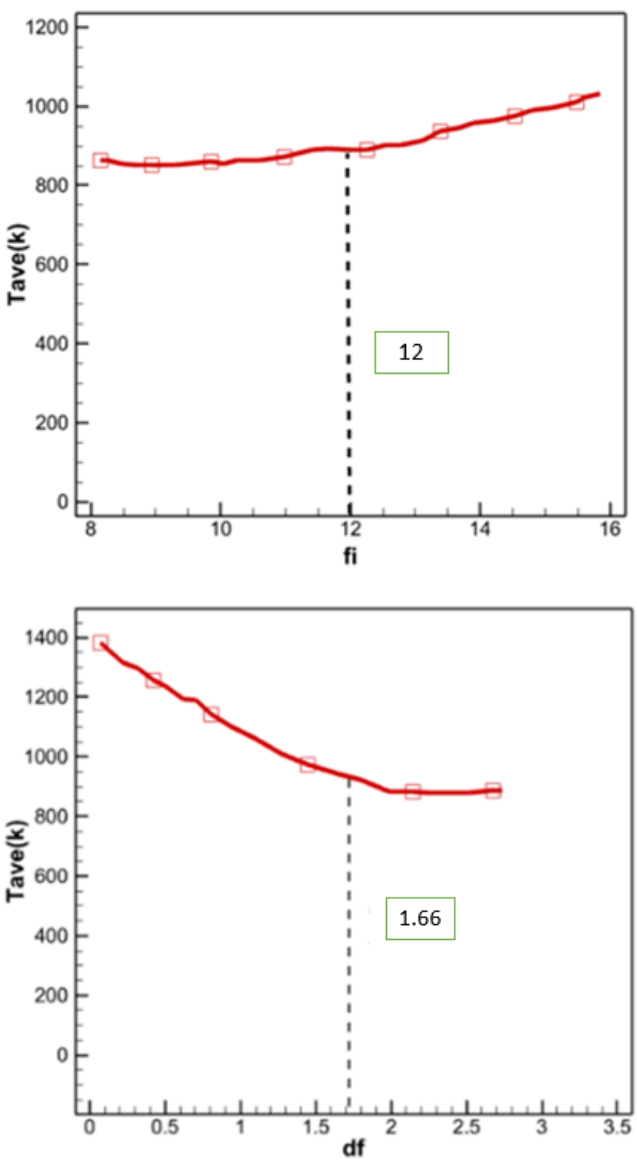


Fig. 12. Changes in the diameter of film cooling holes (df) (right side) and changes in the center-to-center distance of film cooling holes (fi) (left side) in terms of Tave for the blowing ratio of 0.5

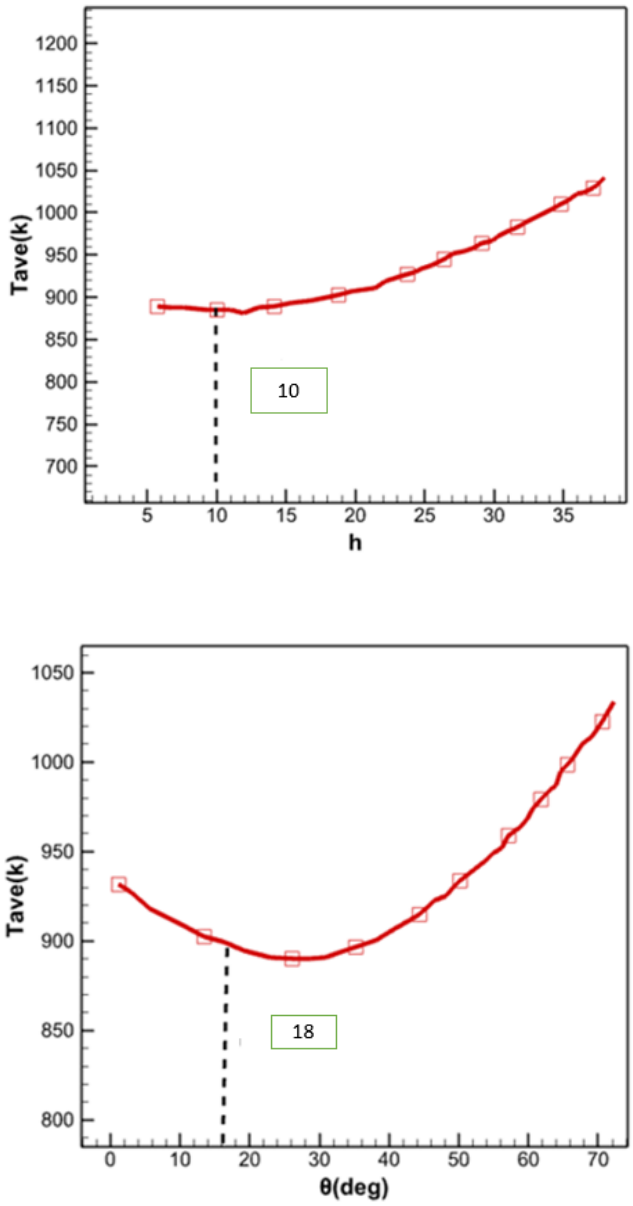


Fig. 13. Changes in the distance between two film-impingement cooling plates (h) (right side) and changes in the film cooling angle (θ) in terms of Tave for the blowing ratio of 0.5

Table 5. Specifications of the optimal geometry with the highest cooling efficiency for the blowing ratio 1

| M | N | $f_i$ (mm) | H (mm) | θ | $d_f$ (mm) | $d_i$ (mm) |
|---|---|---|---|---|---|---|
| 1 | 3 | 12 | 11.542 | 14.69 | 1.6 | 1.0099 |

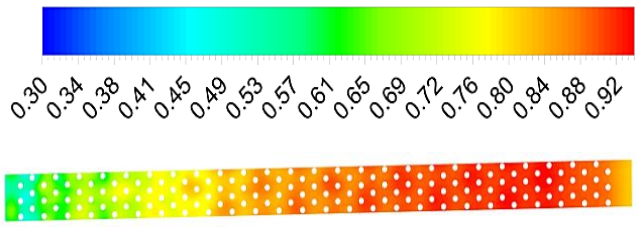


Fig. 14. Contour of cooling efficiency distribution on a flat plate with a blowing ratio of 1

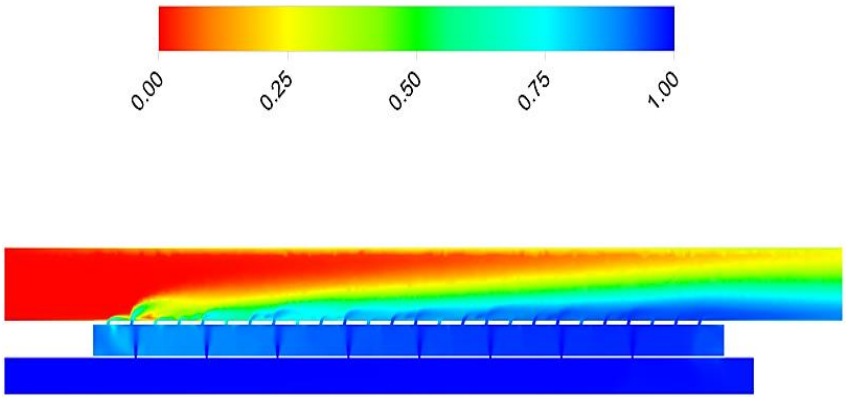


**Fig. 15. Cooling efficiency distribution contour for the optimal geometry with a blowing ratio of 1**

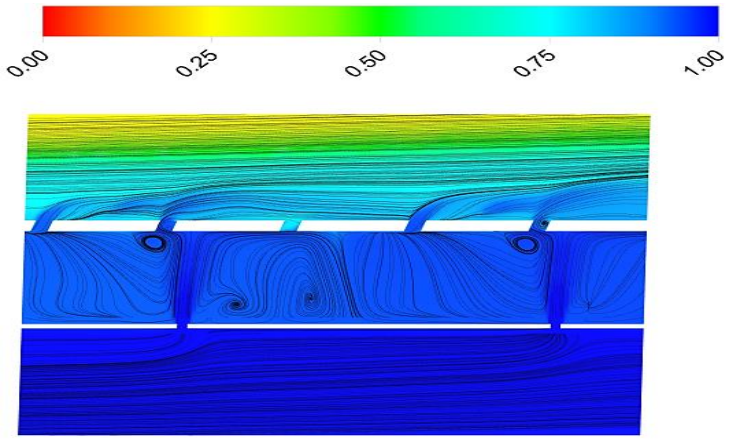


**Fig. 16. Streamline distribution for the optimal geometry with blowing ratio 1**

enters the hot gas flow through the film cooling holes fixed on the flat plate. The range of cooling efficiency is between 0 and 1. In the regions near the injection holes, the cooling efficiency reaches its maximum value. As can be seen, at the beginning of the hot gas flow, the efficiency is zero due to the lack of expansion of the cooling fluid to that area. As the end of the flat plate is approached and the momentum of the cold gas flow increases, effective cooling is achieved, resulting in the attainment of maximum efficiency.

Fig.16 shows the distribution of streamlines for the optimal geometry with a blowing ratio of 1. The angle of the impingement cooling holes is 90 degrees. The cooling fluid enters the hot gas stream through the film cooling holes embedded in the flat plate. The range of cooling efficiency is between 0 and 1, which reaches its maximum value in the areas near the hole. As observed, the presence of vortices near the film cooling holes facilitates the penetration of the cooling fluid into the hot gas flow. The reason for this penetration is the high speed of the cooling fluid, which has overcome the pressure drop created in the holes of the film.

Fig.17 shows the sensitivity of the input parameters in terms of percentage of cooling efficiency ($\eta$) with a blowing ratio of 1. As evident, with the increase in the three parameters of film cooling hole diameter (df), number of film cooling rows *(N)*, and blowing ratio *(M)*, the cooling efficiency ($\eta$) has increased. Furthermore, the increase in the diameter parameters of impingement cooling holes (di), the distance between film-impingement cooling plates *(h)*, the center-to-center distance of film cooling holes *(fi)*, and the angle of film cooling holes *(θ)* has resulted in a decrease in cooling efficiency. The increase of the two parameters of the diameter of the film cooling holes *(df)* and the number of film cooling rows *(N)*, which are caused by the increase in the momentum and the amount of the input flow of the cooling flow, respectively; It has increased cooling efficiency by 30 and 31%, respectively, which have the greatest impact on improving efficiency. Also, the increase in the pressure drop created between the cooling holes of the film, which led to an increase in h, decreased the cooling efficiency by about 7%, which is the most effective parameter on reducing the cooling

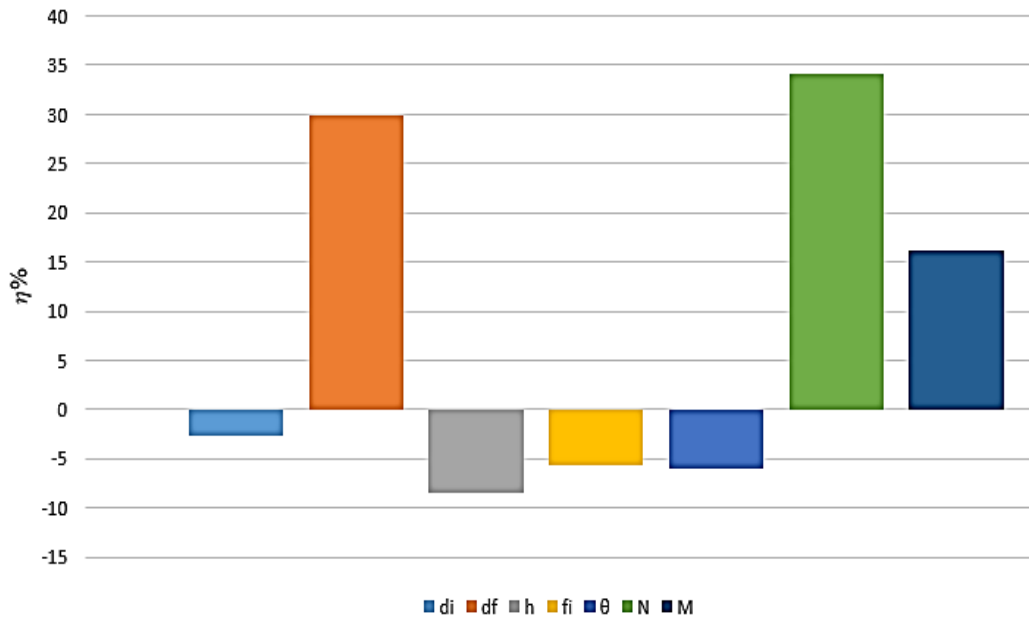


**Fig. 17. The sensitivity of input parameters on cooling efficiency for blowing ratio 1**

efficiency.

Fig.18 illustrates the variations in the diameter of the film cooling holes (df) as well as the center-to-center distance of the cooling holes concerning Tave for a blowing ratio of 1. The results of the optimization have predicted a diameter of 1.6 mm for the optimal geometry with a blowing ratio of 1. As observed, with the increase in df, both the cooling air flow rate and inlet velocity increase, resulting in a decrease in Tave, and consequently, an increase in cooling efficiency. Also, the optimal distance for the center to the center of the cooling holes was chosen to be 12 mm. As observed, initially, with the increase in fi, the high speed of the cooling flow overcomes the created pressure drop, leading to a decrease in Tave, and consequently, an increase in cooling efficiency. Then, with the increase of fi, Tave increases, as a result of which the cooling efficiency has decreased. The reason for this is the increase in the pressure drop created between the cooling holes of the film and the decrease in the momentum of the cooling fluid.

Fig.19 shows the changes in the distance between the two film-impingement cooling plates *(h)* and the changes in the film cooling angle *(θ)* in terms of Tave for the blowing ratio of 1. The results of the optimization have predicted the distance between the two film-impingement cooling plates to be 11.542 mm for the optimal geometry with a blowing ratio of 1. As can be seen, with the increase of h, Tave increases, and consequently the cooling efficiency decreases. Is. The reason for this phenomenon is the increase in pressure drop along the cooling flow path. Also, the cooling efficiency has decreased to a lower value compared to the blowing ratio of 0.5. The reason for this is the heightened momentum of the cooling flow at a blowing ratio of 1 compared to a blowing ratio of 0.5. The optimal angle obtained is also 14.69 degrees. As evident, from an angle of 0 to nearly 30 degrees, Tave has decreased, consequently leading to an increase in cooling efficiency. The reason for this is the remaining flow inside the boundary layer. Then, with an increase in the angle beyond approximately 30 degrees, Tave increases, leading to a decrease in cooling efficiency. The reason for this decrease is the cooling flow directed out of the boundary layer.

In Table 6, you can see the specifications of the optimal geometry with the highest cooling efficiency for the blowing ratio of 1.5. The optimized geometry has 3 rows of film cooling holes. The diameter of the film cooling and impact holes are 1.8481 and 1.3088 mm, respectively. In the optimal geometry, the angle of the film cooling holes is 13.273 degrees and the distance between the two cooling plates is 14.855 mm, which has resulted in a cooling efficiency of 88.7.

Fig.20 shows the cooling efficiency distribution contour on the flat plate for the blowing ratio of 1.5. The range of cooling efficiency is between 0.33 and 0.95, with the minimum and maximum cooling efficiency corresponding to the beginning and end of the flat plate, respectively. As observed, at the initial section of the flat plate, the penetration of cold gas flow is insufficient, resulting in a lower cooling efficiency at the beginning of the flat plate. Then, by approaching the

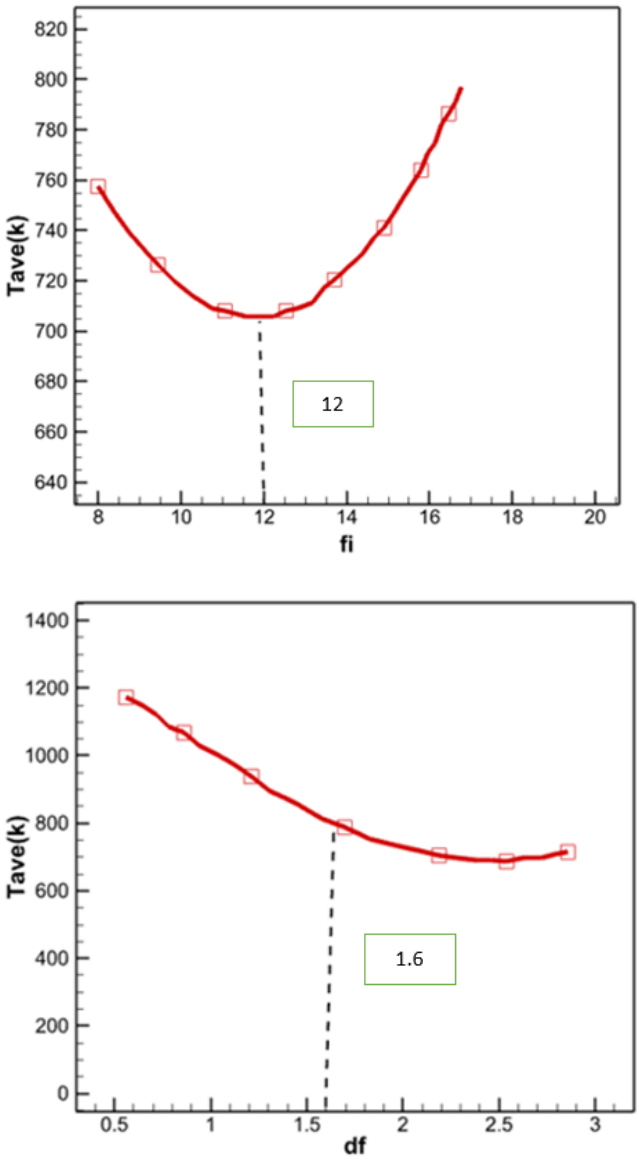


**Fig. 18. Changes in the diameter of the cooling holes of the film (right side) and the distance from the center to the center of the cooling holes (left side) in terms of Tave for the blowing ratio 1**

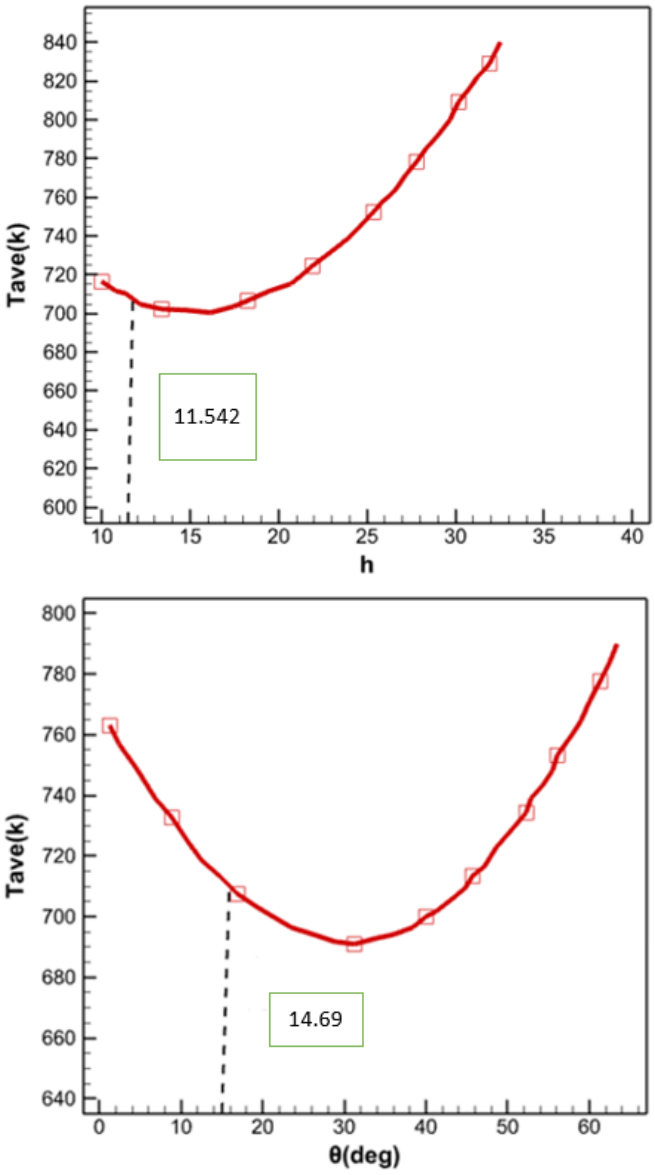


**Fig. 19. Changes in the distance between the two film-collision cooling plates (right side) and changes in the cooling angle (left side) in terms of Tave for the blowing ratio 1**

end of the plate and increasing the flow rate of the cooling fluid, the momentum of the cold gas flow increased, as a result of which the cooling efficiency improved. Similarly, at the trailing edge of the flat plate, the cooling efficiency has slightly decreased. The reason for this is the mixing of the cooling fluid with the hot gas flow, which leads to a partial loss of the cooling fluid's cooling properties.

Fig.21 shows the cooling efficiency distribution for the optimized geometry with a blowing ratio of 1.5. The angle of the impingement cooling holes is 90 degrees. The cooling fluid enters the hot gas flow through the film cooling holes fixed on the flat plate. The range of cooling efficiency is between 0 and 1. In the regions near the injection holes, the cooling efficiency reaches its maximum value. As can be seen, at the beginning of the hot gas flow, the efficiency is zero due to the lack of expansion of the cooling fluid to that area. As the end of the flat plate is approached and the momentum of the cold gas flow increases, effective cooling is achieved, resulting in the attainment of maximum efficiency.

Fig.22 shows the distribution of streamlines for the optimal geometry with a blowing ratio of 1.5. The angle of the impingement cooling holes is 90 degrees. The cooling

**Table 6. Specifications of the optimal geometry with the highest cooling efficiency for the blowing ratio of 1.5**

| M | N | $f_i$ (mm) | H (mm) | θ | $d_f$ (mm) | $d_i$ (mm) |
|---|---|---|---|---|---|---|
| 1.5 | 3 | 13 | 14.855 | 13.273 | 1.8481 | 1.3088 |

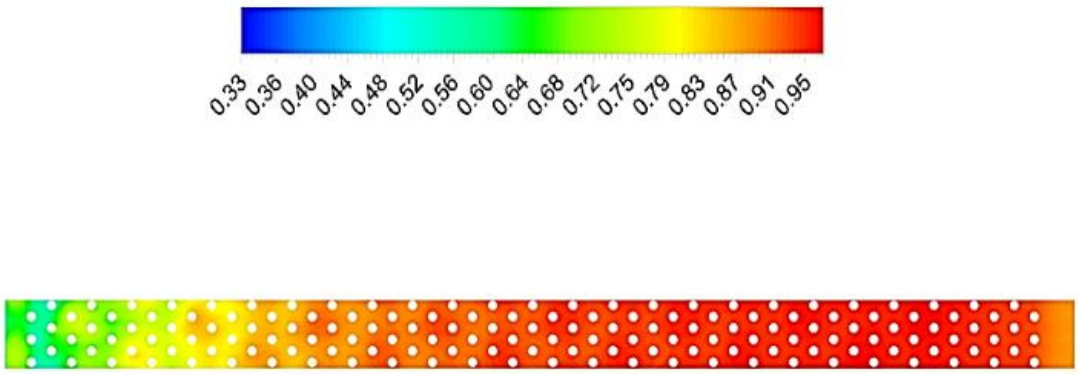


**Fig. 20. Cooling efficiency distribution contour on a flat plate with a blowing ratio of 1.5**

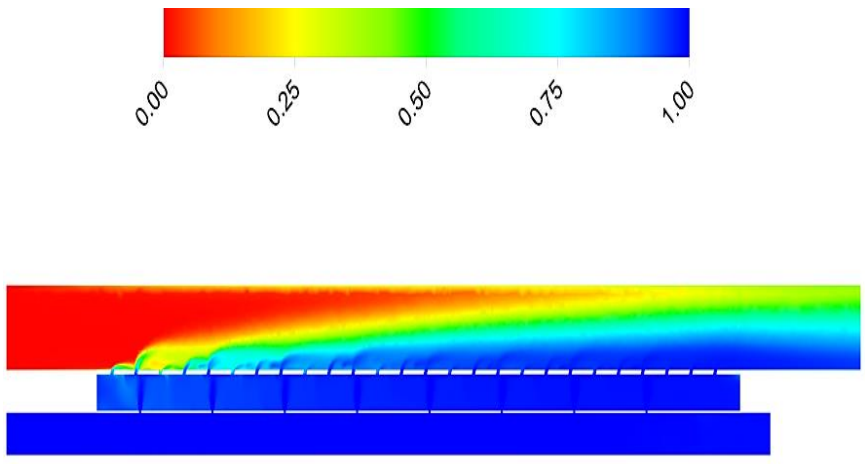


**Fig. 21. Cooling efficiency distribution contour for optimal geometry with 1.5 blowing ratio**

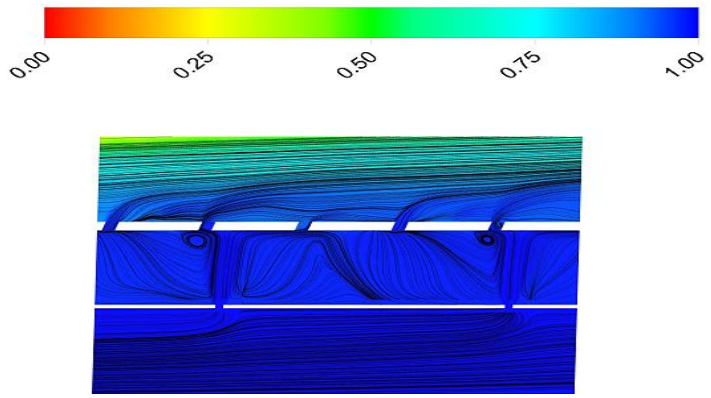


**Fig. 22. Distribution of flow lines for the optimal geometry with a blowing ratio of 1.5**

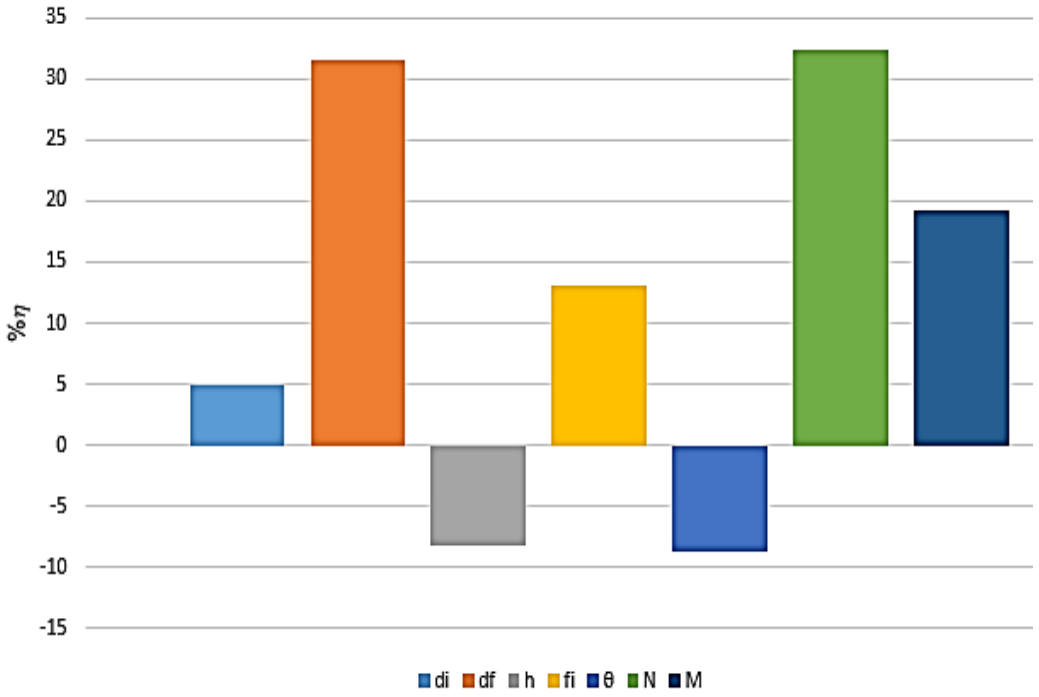


**Fig. 23. The sensitivity of the input parameters on the cooling efficiency for the blowing ratio of 1.5**

fluid enters the hot gas stream through the film cooling holes embedded in the flat plate. The range of cooling efficiency is between 0 and 1, which reaches its maximum value in the areas near the hole. As can be seen, despite the production of small vortices near the cooling holes of the film, the penetration of the cold gas flow into the hot gas has taken place. The reason for this is the high speed of the cooling fluid, which has increased the momentum of the cold gas flow.

Fig.23 shows the sensitivity of the input parameters in terms of the percentage of cooling efficiency ($\eta$) with the blowing ratio of 1.5. As can be seen, by increasing the five parameters of the diameter of film cooling holes *(df)*, number of film cooling rows *(N)*, blowing ratio *(M)*, diameter of impingement cooling holes *(di)*, and center-to-center distance of film cooling holes *(fi)*, the cooling efficiency ($\eta$) has increased. Also, increasing the distance between the film-impingement cooling plates *(h)* and the angle of the film cooling holes *(θ)* has led to a decrease in the cooling efficiency. The increase of the two parameters of the diameter of the film cooling holes *(df)* and the number of film cooling rows *(N)*, which are caused by the increase in the momentum and the amount of the input flow of the cooling flow, respectively; It has increased cooling efficiency by 32 and 33%, respectively, which have the greatest impact on improving efficiency. Also, the increase in pressure drop

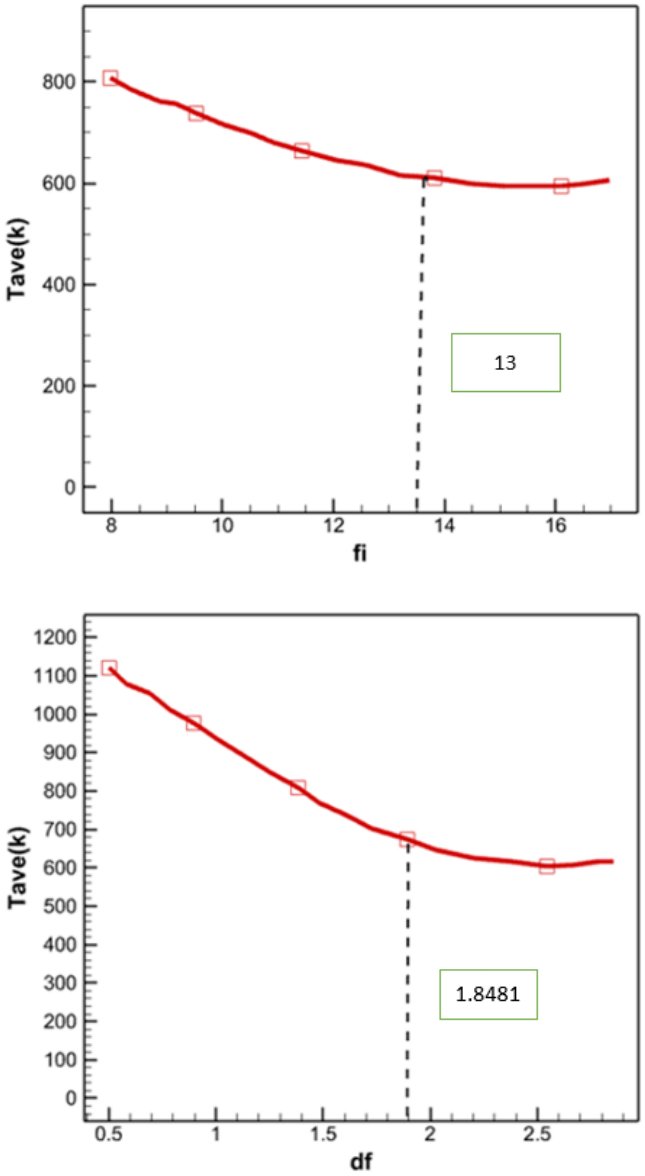


**Fig. 24. Changes in the diameter of the cooling holes of the film (right side) and changes in the center-to-center distance of the cooling holes (left side) in terms of Tave for the blowing ratio of 1.5**

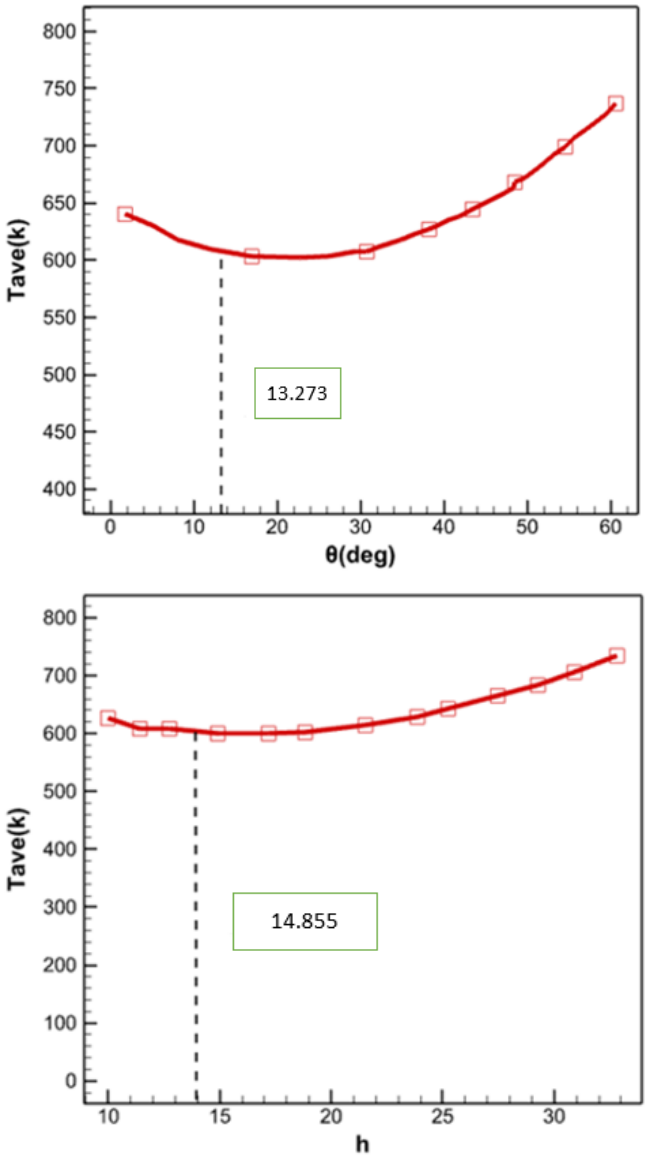


**Fig. 25. Changes in the center-to-center distance of film cooling holes (right side) and changes in the cooling angle (left side) in terms of Tave for the blowing ratio of 1.5**

created between the cooling holes of the film, which led to an increase in h, has reduced the cooling efficiency by about 6%.

Fig.24 shows the changes in the diameter of film cooling holes *(df)* and the center-to-center distance of film cooling holes *(fi)* in terms of Tave for the blowing ratio of 1.5. The results of the optimization have predicted a diameter of 1.8481 mm for the optimal geometry with a blowing ratio of 1.5. As observed, with the increase in df, both the cooling air flow rate and inlet speed increase, leading to a decrease in Tave, and consequently, an increase in cooling efficiency. Also, 13 mm was predicted for the optimal distance of the cooling holes. As observed, with the increase in fi , the high speed and momentum of the cooling fluid enable it to overcome the pressure drop, resulting in a reduction in Tave, and consequently, an increase in cooling efficiency.

Fig.25 shows the changes in the distance between the two film-impingement cooling plates *(h)* and the changes in the film cooling angle in terms of Tave for the blowing ratio of 1.5. The results of the optimization have predicted the distance between the two film-impingement cooling plates to be 14.855 mm for the optimal geometry with a blowing ratio of 1.5. As can be seen, as h increases, Tave increases, and

cooling efficiency decreases. The reason for this reduction is the increase in pressure drop along the cooling flow path. Also, the cooling efficiency has decreased to a lesser amount compared to the blowing ratios of 0.5 and 1. The reason for this reduction is the heightened momentum of the cooling flow at a blowing ratio of 1.5 compared to blowing ratios of 0.5 and 1. Also, the optimum cooling angle for this geometry is 13.273 degrees. As evident, from an angle of 0 to nearly 20 degrees, Tave decreased, consequently leading to an increase in cooling efficiency. The reason for this increase is the remaining cooling flow inside the boundary layer. Then, with an increase in the angle beyond approximately 20 degrees, Tave increased, leading to a decrease in cooling efficiency. The reason for this reduction is the diversion of the cooling flow out of the boundary layer.

Based on the results obtained in this research, each of the optimized geometries in the three blowing ratios of 0.5, 1, and 1.5 have three rows of film cooling. In the three optimized geometries, the two parameters of the film cooling hole diameter *(df)* and the number of film cooling rows *(N)* have the greatest effect on increasing the cooling efficiency. Additionally, in the optimal geometries, at the onset of the flat plate, inadequate cold gas flow results in inefficient cooling, while approaching the end of the plate enhances cooling efficiency. Also, in all three geometries, the cooling efficiency has decreased by increasing the distance between the film-impingement cooling holes *(h)*. In the blowing ratios of 0.5 and 1, the cooling efficiency has decreased by increasing the center-to-center distance of film cooling holes *(fi)* and increasing the diameter of impingement cooling holes *(di)*; But in the blowing ratio of 1.5, the cooling efficiency has been improved by increasing the center-to-center distance of the cooling holes of the film *(fi)*. In the ratio of 0.5 and 1.5 blowing, the cooling efficiency increased from 0 to about 20 degrees, and from about 20 degrees onwards, the cooling efficiency decreased. In the case of a blowing ratio of 1, the cooling efficiency has increased from 0 to approximately 30 degrees, but beyond 30 degrees, the cooling efficiency has decreased. Additionally, the cooling efficiency has increased with the rise in the blowing ratio. One of the reasons is the increase in the momentum of the cooling fluid. According to the mentioned contents, the blowing ratio of 1.5 has the best performance for cooling. The reason for this is the increase in cooling efficiency compared to the blowing ratios of 0.5 and 1.

## 5- Conclusion

Considering the increasing use of turbine engines, the study of flow and heat transfer in them is very important. There are different types of air turbine engines. In a general view, each of these engines can be divided into cold and hot sections. The hot components of these engines encompass the rows of high-pressure compressor blades, combustion chamber, afterburner, and nozzle. Enhancing the efficiency of turbine engines necessitates augmenting the turbine inlet temperature and bolstering the thrust force, often mandating re-ignition through the utilization of afterburners. In both cases, the temperature of the engine exhaust gases will increase significantly. Accordingly, the technology of the cooling systems of the nozzle walls is of great importance. In this research, the analysis and optimization of the cooling system for converting a circular to a rectangular duct in a turbine engine have been conducted. The optimization of the transition duct has been accomplished utilizing a genetic algorithm in conjunction with Fluent computational fluid dynamics software. The following results can be enumerated for the analysis and optimization of the cooling system of the circular to a rectangular duct transition in a turbine engine:

- By enlarging the diameter of the film cooling apertures, efficiency is enhanced due to the heightened momentum of the cooling flow.
- The augmentation in blowing ratio resulting from the escalated flow velocity across the cooling plate has contributed to the enhancement of cooling efficiency.
- Increasing the spacing between the film-impingement cooling plates results in a decrease in cooling efficiency. This is attributable to the diminished momentum of the cooling flow caused by the elevated pressure drop along the flow path.
- Cooling initiation is absent at the onset of the flat plate, attributed to the inadequate fluid expansion into the regions preceding the cooling apertures.
- At a blowing ratio of 0.5, the effective penetration of the cooling fluid into the hot gas flow is inadequate. This can be attributed to the generation of swirl near the film cooling orifices.
- At a blowing ratio of 0.5, enhancing both the diameter of the film cooling apertures and the number of film cooling rows has resulted in a 30% increase in cooling efficiency with the former and a 28% increase with the latter.
- At a blowing ratio of 1, augmenting both the diameter of the film cooling apertures and the number of cooling rows has led to a 30% improvement in cooling efficiency with the former and a 31% improvement with the latter.
- In the blowing ratio of 1.5, the diameter of the film cooling holes and the number of cooling rows have improved the cooling efficiency by 32 and 33%, respectively.
- In the ratio of 0.5 and 1.5 blowing, the cooling efficiency has increased up to the angle of 20 degrees, and from the angle of 20 degrees onwards, the cooling efficiency has decreased.
- At the blowing ratio of 1 up to the angle of 30 degrees, the cooling efficiency has increased, and from the angle of 30 degrees onwards, the cooling efficiency has decreased.
- The blowing ratio of 1.5 has the highest cooling efficiency and has the best performance.

## References

[1] J. Niu, C. Liu, H. Liu, X. Xiao, J. Lin, Theoretical and experimental analysis of overall cooling effectiveness for afterburner double-wall heat shield, International Journal of Heat and Mass Transfer, 176 (2021) 121360.

[2] Y. Jia, Y. Liu, Z. Meng, W. Yin, W. Hua, Numerical study on film cooling effectiveness from spiral-channel hole, International Communications in Heat and Mass

Transfer, 143 (2023) 106716.

[3] R.D. Plant, J. Friedman, M.Z. Saghir, A review of jet impingement cooling, International Journal of Thermofluids, 17 (2023) 100312.

[4] D.E. Metzger, R.S. Bunker, Local heat transfer in internally cooled turbine airfoil leading edge regions: Part II-impingement cooling with film coolant extraction, (1990) 459-466.

[5] V.K. Garg, R.E. Gaugler, Effect of velocity and temperature distribution at the hole exit on film cooling of turbine blades, American Society of Mechanical Engineers, (1997) 343-351.

[6] D. Walters, J. Leylek, A systematic computational methodology applied to a three-dimensional film-cooling flowfield, (1997) 777-785.

[7] S. Baldauf, A. Schulz, S. Wittig, High-resolution measurements of local effectiveness by discrete hole film cooling, 123(4) (2001) 758-765.

[8] R. Kaszeta, T.W. Simon, Measurement of eddy diffusivity of momentum in film cooling flows with streamwise injection, J. Turbomach., 122(1) (2000) 178-183.

[9] F. Bazdidi-Tehrani, A.A. Mahmoodi, Investigation of the effect of turbulence intensity and injection angle on the flow and temperature field in the single hole film cooling technique, International Journal of Engineering Science, 4 (2002).

[10] S. Zecchi, L. Arcangeli, B. Facchini, D. Coutandin, Features of a cooling system simulation tool used in the industrial preliminary design stage, Turbo Expo: Power for Land, Sea, and Air, 41685 (2004) 493-501.

[11] J.E. Albert, D.G. Bogard, F. Cunha, Adiabatic and overall effectiveness for a film cooled blade, Turbo Expo: Power for Land, Sea, and Air, 41677 (2004) 251-259.

[12] M. Ghorab, S.I. Kim, I. Hassan, Conjugate heat transfer and film cooling of a multi-stage cooling scheme, ASME International Mechanical Engineering Congress and Exposition, 48715 (2008) 1249-1257.

[13] L.D. Dobrowolski, D.G. Bogard, J. Piggush, A. Kohli, Numerical simulation of a simulated film cooled turbine blade leading edge including conjugate heat transfer effects, ASME International Mechanical Engineering Congress and Exposition, 43826 (2009) 2145-2156.

[14] S. Ravelli, L. Dobrowolski, D.G. Bogard, Evaluating the effects of internal impingement cooling on a film cooled turbine blade leading edge, Turbo Expo: Power for Land, Sea, and Air, 43994 (2010) 1655-1665.

[15] B. Suresh, A. Brijesh, V. Kesavan, S.K. Kumar, Heat Transfer and Flow Studies of Different Cooling Configurations for Gas Turbine Rotor Blade, in: Gas Turbine India Conference, American Society of Mechanical Engineers, 49644 (2014), V001T004A006.

[16] S.R. Klavetter, J.W. McClintic, D.G. Bogard, J.E. Dees, G.M. Laskowski, R. Briggs, The effect of rib turbulators on film cooling effectiveness of round compound angle holes fed by an internal cross-flow, Journal of Turbomachinery, 138(12) (2016) 121006.

[17] J. Wang, B. Sunden, H. Wu, J. Yang, C. Gu, Q. Wang, Conjugated heat transfer analysis of a film cooling passage with turbulator ribs, Heat Transfer Research, 47(2) (2016).

[18] B. Zhao, M. Hu, X. Ao, N. Chen, G. Pei, Radiative cooling: A review of fundamentals, materials, applications, and prospects, Applied energy, 236 (2019) 489-513.

[19] A. Radchenko, E. Trushliakov, K. Kosowski, D. Mikielewicz, M. Radchenko, Innovative turbine intake air cooling systems and their rational designing, Energies, 13(23) (2020) 6201.

[20] T. Jackowski, M. Elfner, H.-J. Bauer, Experimental study of impingement Effusion-Cooled Double-Wall combustor liners: thermal analysis, Energies, 14(16) (2021) 4843.

[21] S. Fan, W. Li, Photonics and thermodynamics concepts in radiative cooling, Nature Photonics, 16(3) (2022) 182-190.

[22] J. Zhang, Q. Zheng, J. Xu, G. Yue, Y. Jiang, Conjugate heat transfer and flow analysis on double-wall cooling with impingement induced swirling and film cooling, Applied Thermal Engineering, 223 (2023) 120014.

[23] A. ANSYS FLUENT, Fluent Theory Guide, (2013).

**HOW TO CITE THIS ARTICLE**

*B. Shahriari, M. Dehghani, P. Hashemi, M. Mohamad Hassanzade, Optimization of cooling system of circular to rectangular transition duct in a turbine engine nozzle, AUT J. Mech Eng., 9(2) (2025) 123-142.*

**DOI:** 10.22060/ajme.2025.23303.6120